Acod1-mediated inhibition of aerobic glycolysis suppresses osteoclast differentiation and attenuates bone erosion in arthritis

SUPPLEMENTAL MATERIAL

Supplemental methods

Viability Dye staining

Cells were harvested from the plate upon incubation with 0.5 mM EDTA in 1x PBS for 10 min at 37°C, washed and stained with zombie violet fixable viability dye (Biolegend) for 30 min at 4°C in the dark.

Mass spectrometry

For the detection of 4-OI in in vitro differentiated murine osteoclasts, $4x10^6$ BMMs were plated at a cell density of $1x10^6$ cells per 1000 µl and differentiated into osteoclasts as described in the respective section. Mature osteoclasts were lysed in ice-cold 80% methanol containing recovery standards and analyzed by liquid chromatography mass spectrometry (LC-MS) as previously described[1 2]. Briefly, extraction samples were centrifuged for 5 min at 16000 rpm and 4 °C and the supernatants were distributed into 2 separate LC vials. Aliquots from all samples were furthermore pooled and the sample mix was used for quality control (QC), undergoing the same procedure as the individual samples. All samples and QCs were dried using a nitrogen stream at RT. Samples were then reconstituted with eluent for hydrophilic interaction liquid chromatography (HILIC) or reverse phase liquid chromatography (RP) following transfer into HPLC insert vials. LC-MS analysis was performed on a Dionex Ultimate 3000 chromatographic system coupled to a Q Exactive Focus mass spectrometer (both from Thermo Fisher Scientific). Recording, processing and evaluation of raw data were accomplished using Trace Finder Software V.4.1 (Thermo Fisher Scientific).

For the detection of itaconate in human PBMCs and in vitro differentiated murine osteoclasts, metabolites were extracted using perchloric acid and analyzed as previously described[3]. Briefly, 8 to $20x10^6$ PBMCs were pelleted and resuspended in 1 ml of ice cold 1 M perchloric acid, followed by addition of 1 ml of 0.1 M perchloric acid. For the analysis of murine osteoclasts, cells were harvested from the plate using 1 ml of ice cold 1 M perchloric acid followed by addition of 1 ml of 0.1 M perchloric acid. The lysates were vortexed and snap frozen using liquid nitrogen. After thawing, lysates were centrifuged for 30 min at 14000 rpm and 4 °C, the supernatants were transferred into new tubes and supplemented with 50 µl of 5 M K_2CO_3, followed by pH-adjustment to 7 and another centrifugation for 5 min at 14000 rpm

Kachler K, *et al. Ann Rheum Dis* 2024; 83:1691–1706. doi: 10.1136/ard-2023-224774

and 4 °C. The supernatants were collected and stored at -80 °C. The extracts were filtered through a 10-kD filter (AcroPrep Omega 10 K; Pall Corporation) prior to analysis by ion chromatography using an ICS3000 HPLC-system (Dionex) connected to a QTrap 3200 Triple-Quadrupole mass spectrometer with turboV ion source (Applied Biosystems) operated in multiple reaction monitoring mode.

Hif1α protein measurement by MSD Kit

BMMs were plated in 12-well plates at a cell density of 2×10^6 cells/ well in 2 ml and cultured under osteoclast differentiating conditions as described in the respective section. On day 3 of cell differentiation, cells were stimulated with 100 µM of $CoCl_2$ for 6 h at 37°C and 5.5 % CO_2 followed by the measurement of Hif1α protein levels using the HIF-1α Whole Cell Lysate Kit (MESO SCALE DIAGNOSTICS) according to manufacturer´s instructions. Briefly, cells were lysed through a 30 min incubation with Tris Lysis Buffer containing proteinase inhibitors on ice. Protein concentration was measured with the DC Protein Assay Kit (Bio-Rad) according to the manufacturer's protocol. The measurement of Hif1α protein level was performed with whole cell lysates containing 6 µg of total protein. The signal intensity was measured via the MSD SECTOR imager.

Evaluation of gene editing efficiency by T7 Endonuclease I assay

The efficiency of CRISPR/ Cas9-mediated *Hif1a* knockout in osteoclasts was assessed via the T7 Endonuclease I assay. Therefore, genomic DNA was extracted using the RNeasy Plus Mini Kit (Quiagen) followed by PCR amplification of the target region surrounding the site of the CRISPR/ Cas9-induced double strand break with Phusion High-Fidelity DNA Polymerase (New England Biolabs) and the following primers (forward: 5´-GCCATCTTTCCAGCTCCCCTTA-3´, reverse: 5´-GCAGTACCACAGCAAGAAGTCAG-3´). PCR products were purified via the PCR Purification Kit (Quiagen), denatured at 95°C for 5 min and re-annealed through gradual cooling to 85°C with a 2°C temperature decrease per second, followed by a 0.1°C temperature decrease per second to 25°C. The PCR products were then digested with T7-Endonuclease I (New England Biolabs) at 37°C for 15 min and loaded onto 2 % agarose gel for separation. Knockout efficiency was determined by analyzing the band intensity of digested DNA heteroduplexes relative to the naïve band intensity using ImageJ software.

Kachler K, *et al. Ann Rheum Dis* 2024; 83:1691–1706. doi: 10.1136/ard-2023-224774

Supplemental tables

Table S1: qPCR primers for human genes

Gene	Forward sequence	Reverse sequence
ACOD1	5´-GTGTTTCACATAGCCAGCCAA-3´	5´-AGTGAATAGCCACACCGTTCA-3´
B2M	5´-GATGAGTATGCCTGCCGTGTG-3´	5´-CAATCCAAATGCGGCATCT-3´
SLC2A1	5´-GTCTGGCATCAACGCTGTCT-3´	5´-AACAGCGACACGACAGTGAA-3´
ALDOC	5´-CAGTGCTGATGACCGTGTGA-3´	5´-CACCCTTGTCAACCTTGATGC-3´
PGK1	5´-GTTGACCGAATCACCGACCT-3´	5´-GTCGACTCTCATAACGACCCG-3´
ENO1	5´-ACAACCAGCTCCTCAGAATTGAA-3´	5´-GGTCTGTGTAGCCAACAGGT-3´
LDHA	5´-CTTGACCTACGTGGCTTGGA-3´	5´-CTCCATACAGGCACACTGGAA-3´
PDK1	5´-AGGAGGTGGCGTTCCTTTG-3´	5´-CCATAACCAAAACCAGCCAGAG-3´
NFATC1	5´-GTCCTGTCTGGCCACAAC-3´	5´-GGTCAGTTTTCGCTTCCATC-3´
ACP5	5´-TGAGGACGTATTCTCTGACCG-3´	5´-CACATTGGTCTGTGGGATCTTG-3´
MMP9	5´-CCTGGAGACCTGAGAACCAA-3´	5´-ATTTCGACTCTCCACGCATC-3´
CTSK	5´-TTCCCGCAGTAATGACACCC-3´	5´-GGAACCACACTGACCCTGAT-3´

Table S2: qPCR primers for murine genes

Gene	Forward sequence	Reverse sequence
Actb1	5´-TGTCCACCTTCCAGCAGATGT-3´	5´-AGCTCAGTAACAGTCCGCCTAGA-3´
Tnfrsf11a	5´-CCCTTGCAGCTCAACAAGGATACG-3´	5´-CTTTCCAAGGAGGGTGCAGTTGG-3´
Acp5	5´-CGACCATTGTTAGCCACATACG-3´	5´-TCGTCCTGAAGATACTGCAGGTT-3´
Ctsk	5´-CACCCTTAGTCTTCCGCTCA-3´	5´-CTTGAACACCCACATCCTGCT-3´
Tcirg1	5´-GCTCATGGGTCTGTTCTCCG-3´	5´-CAGATACTCGTCACTCCAGCC-3´
Calcr	5´-CATGGCTGTGTTTACCGACG-3´	5´-CTCAGCCAGCAGTTGTCGTT-3´
Slc2a1	5´-TTAATCGCTTTGGCAGGCGG-3´	5´-CCCAGTTTGGAGAAGCCCAT-3´
Ldha	5´-CCAGCAAAGACTACTGTGTAACTG-3´	5´-AGATGTTCACGTTTCGCTGGA-3´
Aldoc	5´-GGCAGAGATGAACGGGCTTG-3´	5´-GGCGATGTAGAGGGACTGTG-3´
Dnm1l	5´-GCGGATATGCTGAAGGCATTAC-3´	5´-GTAGGCAGCAGCAGGTTCAA-3´
Nfatc1	5´-GGTGCCTTTTGCGAGCAGTATC-3´	5´-CGTATGGACCAGAATGTGACGG-3´
Traf6	5´-AAAGCGAGAGATTCTTTCCCTG-3´	5´-ACTGGGGACAATTCACTAGAGC-3´
Mmp9	5´-GCTGACTACGATAAGGACGGCA-3´	5´-TAGTGGTGCAGGCAGAGTAGGA-3´

Kachler K, *et al. Ann Rheum Dis* 2024; 83:1691–1706. doi: 10.1136/ard-2023-224774

Supplemental Figure legends

Supplemental Figure 1: Negative correlation between itaconate levels and disease activity in RA patients. (A) Aconitate decarboxylase 1 (*ACOD1)* mRNA expression level in peripheral blood mononuclear cells (PBMCs) from healthy donors (HD) and rheumatoid arthritis (RA) patients with active RA and remission, presented as fold changes (n=8-15). **(B)** Mass spectrometry analysis of itaconate levels in PBMCs, isolated from the blood of RA patients with active disease or remission and HD (n=8-13). **(C)** Correlation between the mRNA expression level of *ACOD1* and itaconate level in PBMCs from patients with RA (n=18). **(D)** Correlation between the level of itaconate in PBMCs from patients with RA and the corresponding disease activity score DAS28 (n=21). **(E)** Quantification and **(F)** representative images of tartrate resistant acid phosphatase (TRAP)-positive, polynucleated (≥ 3 nuclei) human osteoclasts, derived from PBMCs of HD in the presence of the indicated doses of 4-octyl-itaconate (4-OI) (n=6, with 2 donors and 3 technical replicates per donor). Scale bar: 250µm. **(G)** mRNA expression analysis of osteoclast marker genes in mature human osteoclasts (day 7-9 of in vitro cell culture), derived from HD and RA donor PBMCs and cultured in the presence or absence of 50 µM 4-OI and presented as fold change values (n=3-4). Data are shown as mean ± SEM. Symbols represent individual donors. P-values were determined by 1-way or 2-way ANOVA for multiple comparisons. Correlations were tested using the linear regression *F* test.

Supplemental Figure 2: Acod1 deficiency alters metabolic profile but not the number of OCPs in experimental arthritis. (A) Proportional ankle joint swelling in wildtype (WT) and aconitate decarboxylase 1-deficient ($Acod1^{-/-}$) mice over the course of K/BxN serum induced arthritis (SIA) (n=21-23). **(B)** mRNA expression analysis of osteoclast marker genes in paw tissue samples from WT and $Acod1^{-/-}$ mice with SIA, presented as fold change values (n=15-22). **(C)** Gating strategy for flow cytometry analysis of $CD115^{+}Ly6C^{hi}CD11b^{+}CD45^{+}$ osteoclast precursor cells (OCPs) in synovial tissue samples. **(D)** Quantification of OCP percentage gated on $CD45^{+}$ cells in the synovial ankle tissue of WT naïve, WT SIA and $Acod1^{-/-}$ SIA mice (n=19-20). **(E)** Representative images of tartrate resistant acid phosphatase (TRAP) staining on tibiae from naïve WT and $Acod1^{-/-}$ mice. White arrow heads indicate osteoclasts. Scale bar: 50 µm. **(F)** Quantification of bone volume per total volume (BV/TV), trabecular thickness (Tb.Th), trabecular number (Tb.N), trabecular space (Tb.Sp), number of osteoclasts per bone perimeter (N.Oc/B.Pm) and osteoclast surface per bone surface (Oc.S/BS) (n=11-14). **(G)** Gating strategy for SCENITH analysis in ankle-resident OCPs. **(H)** Quantification of puromycin mean fluorescence intensity (MFI) levels in ankle-resident OCPs from WT naïve, WT SIA and $Acod1^{-/-}$ SIA mice after the administration of the metabolic modulators 2-deoxy-D-glucose (DG), oligomycin (O) and DG and O as compared to unstimulated control (Co) (n=4-5). Data are shown as mean ± SEM. Symbols represent individual mice. P-values were determined by 2-tailed Student´s *t* test for single comparisons and 1-way or 2-way ANOVA for multiple comparisons.

Supplemental Figure 3: 4-OI stimulation affects osteoclast differentiation, actin-ring formation and gene expression, but not viability. (A) Immunofluorescence microscopy staining of F-actin (red) and DAPI (blue) in wildtype (WT) and aconitate decarboxylase 1-deficient ($Acod1^{-/-}$) osteoclasts (day 3 of cell culture) that were either unstimulated or stimulated with 100 µM 4-octyl-itaconate (4-OI) for 48 h. White arrow heads indicate the F-actin ring. Scale bar: 100 µm. **(B)** Mass spectrometry analysis of Itaconate levels in osteoclasts, differentiated from WT and $Acod1^{-/-}$ bone marrow-derived monocytes (BMMs) (n=3). **(C)** Quantification and **(D)** representative images of tartrate resistant acid phosphatase (TRAP)-positive, polynucleated (≥ 5 nuclei) osteoclasts that were differentiated from WT BMMs in the presence of the indicated doses of 4-OI (n=3). Scale bar: 250 µm. **(E)** Quantification and **(F)** representative images of viability percentage in WT BMMs stimulated with the indicated doses of 4-OI through flow cytometry analysis of viability dye (FVD) staining on day 2 of osteoclast in vitro differentiation (n=2-3). **(G)** Mass spectrometry analysis of 4-OI levels in WT osteoclasts that were cultured in the presence or absence of 100 µM 4-OI, presented as fold changes of the normalized peak area (n=3). **(H)** Principle component analysis (PCA) showing the clustering of RNA sequencing samples from WT CTR, $Acod1^{-/-}$ CTR and $Acod1^{-/-}$ 4-OI osteoclasts. PC1 explains 79% of the total variance and PC2 explains 10.6% of the total variance. **(I)** Volcano plot showing the differentially expressed genes between $Acod1^{-/-}$ CTR and WT CTR osteoclasts and between $Acod1^{-/-}$ 4-OI and $Acod1^{-/-}$ CTR osteoclasts with a p-value cutoff of 0.05 and an absolute log2 fold change cutoff of 0.5. Significantly altered genes are illustrated as purple dots. **(J)** Gene set enrichment analysis in $Acod1^{-/-}$ CTR osteoclasts as compared to WT CTR osteoclasts with a p-value cutoff of 0.05 and visualization of the hallmark term “rheumatoid arthritis”. Data are shown as mean ± SEM. Symbols represent individual mice. P-values were determined by 2-tailed Student´s *t* test for single comparisons and 1-way ANOVA for multiple comparisons.

Supplemental Figure 4: Metabolic modification through 2-DG and CCCP alters osteoclast differentiation efficiency. (A) Fold change expression of glycolytic enzyme genes in aconitate decarboxylase 1-deficient (Acod1$^{-/-}$) as compared to wildtype (WT) osteoclasts on day 3 of cell culture (n=6-7). **(B)** Representative images and **(C)** quantification of tartrate resistant acid phosphatase (TRAP)-positive, polynucleated (≥ 5 nuclei) osteoclasts that were differentiated from WT and Acod1$^{-/-}$ bone marrow-derived monocytes (BMMs) after a 3 h stimulation with 2 mM 2-desoxy-D-glucose (2-DG) on day 1 of osteoclast cell culture as compared to unstimulated cells (n=5-6). Scale bar: 100 µm. **(D)** Quantification and **(E)** representative images of viability percentage in WT and Acod1$^{-/-}$ BMMs after stimulation with 2-DG through flow cytometry analysis of viability dye (FVD) staining on day 2 of osteoclast in vitro differentiation (n=4). **(F)** Representative images and **(G)** quantification of TRAP-positive, polynucleated (≥ 5 nuclei) osteoclasts that were differentiated from WT BMMs after a 3 h stimulation with 5 µM cyanide m-chlorophenyl hydrazone (CCCP) on day 1 of osteoclast cell culture as compared to unstimulated cells (n=3 cell replicates from 1 animal). Scale bar: 100 µm. **(H)** Quantification of hypoxia inducible factor 1α (Hif1α) protein level on day 1, 2 and 3 of WT osteoclast in vitro cell culture. The cells were either unstimulated or stimulated with cobalt chloride ($CoCl_2$) for 6 h prior to measurement using the Meso Scale Discovery (MSD) Hif1α whole cell lysate kit (n=3). **(I)** Representative image of agarose gelelectrophoresis following a T7-endonuclease I assay with genomic DNA (gDNA) from Acod1$^{-/-}$ osteoclasts that were derived from BMMs that were transfected with a Cas9 protein and a Hif1α guide RNA (Hif1α sgRNA) or a non-targeting control (NT-CTR). Arrows indicate the position of the uncleaved Hif1α PCR product and the T7 endonuclease digested PCR product fragments. **(J)** Glycolytic activity parameters in osteoclasts (day 3 of cell culture) from Acod1$^{-/-}$ mice that were subjected to CRISPR-Cas9-mediated deletion of Hif1α gene or from WT and Acod1$^{-/-}$ mice that were treated with a non-targeting control construct on day 0 of osteoclast cell culture, determined by glycolytic stress test assay (n=3-5). Data are shown as mean ± SEM. Symbols represent individual mice unless stated otherwise. P-values were determined by 1-way ANOVA or 2-way ANOVA for multiple comparisons.

Supplemental Figure 5: Inhibition of ROS and Sdh-activity mimics the effect of 4-OI on osteoclast differentiation and Hif1α stabilization. (A) Representative images and **(B)** quantification of tartrate resistant acid phosphatase (TRAP)-positive, polynucleated (≥ 5 nuclei) osteoclasts that were differentiated from wildtype (WT) and aconitate decarboxylase 1-deficient (Acod1$^{-/-}$) bone marrow-derived monocytes (BMMs) after stimulation with 0.5 mM of n-acetyl-l-cysteine (NAC) for 48h or 20 mM of dimethyl-malonate (DMM) for 3 h on day 1 and 2 of osteoclast cell culture as compared to unstimulated cells (CTR) (n=4-10). Scale bar: 100 µm. **(C)** Representative images and **(D)** fold change quantification of immunofluorescent staining for hypoxia inducible factor 1α (Hif1α) (yellow), F-actin (purple) and DAPI (blue) in osteoclasts, differentiated from WT and Acod1$^{-/-}$ BMMs after stimulation with NAC or DMM as compared to unstimulated control osteoclasts (n=6). Scale bar: 70 µm. Data are shown as mean ± SEM. Symbols represent individual mice. P-values were determined by multiple paired *t* tests or 2-way ANOVA for multiple comparisons.

Supplemental Figure 6: 4-OI treatment does not affect OCP number in experimental arthritis.
(A) Experimental procedure for K/BxN serum induced arthritis (SIA) in wildtype (WT) mice and therapeutic treatment through intraperitoneal injection of 1 mg 4-octyl-itaconate (4-OI) on day 1, 3, 5 and 7 post K/BxN serum injection. **(B)** Quantification of osteoclast progenitor (OCP) percentage ($CD115^+Ly6C^{hi}CD11b^+CD45^+$ cells), gated on $CD45^+$ cells in the synovial ankle tissue of 4-OI treated and untreated control mice (CTR) with SIA (n=19-20). **(C)** Quantification of puromycin levels in ankle-resident OCPs from 4-OI treated and CTR mice with SIA after the administration of the metabolic modulators 2-deoxy-D-glucose (DG), oligomycin (O) and DG and O as compared to unstimulated control (Co) (n=4-5). Data are shown as mean ± SEM. Symbols represent individual mice. P-values were determined by 2-tailed Student´s *t* test for single comparisons and 1-way ANOVA for multiple comparisons.

Supplemental Figure 7: 4-OI treatment ameliorates inflammation and bone degradation in hTNFtg mice. (A) Experimental procedure for 4-octyl-itaconate (4-OI) treatment of hTNFtg mice. 7 weeks old hTNFtg mice were intraperitoneally injected with 4-OI every 3 days over a total period of 21 days. **(B)** Arthritis score and proportional weight change in 4-OI treated and untreated hTNFtg mice over the course of 21 days (n=3-4). **(C)** Area under the curve for the arthritis score and weight change

measurement in 4-OI treated and untreated hTNFtg mice (n=3-4). **(D)** Fold change of paw and ankle swelling in 4-OI treated as compared to untreated hTNFtg mice on day 21 of the experiment relative to day 0 (n=3-4). **(E)** Representative pictures of Hematoxylin and eosin (H&E) and tartrate resistant acid phosphatase (TRAP)-stained paw tissue sections from 4-OI treated and untreated hTNFtg mice. Black arrow heads (H&E staining) indicate inflammation, blue arrow heads (TRAP staining) indicate eroded bone tissue with osteoclasts. Scale bar: 200 µm. **(F)** Quantification of inflammation area (I.Ar), eroded area (E.Ar) and osteoclast number (N.Oc) in H&E and TRAP-stained paw tissue sections of 4-OI treated and untreated hTNFtg mice (n=3-4). **(G)** Representative images of TRAP-stained tibial sections from wildtype (WT) mice, 4-OI treated and untreated hTNFtg mice. White arrow heads indicate osteoclasts. Scale bar: 50 µm. **(H)** Quantification of bone volume per total volume (BV/TV), trabecular thickness (Tb.Th), trabecular number (Tb.N), trabecular space (Tb.Sp), number of osteoclasts per bone perimeter (N.Oc/B.Pm) and osteoclast surface per bone surface (Oc.S/BS) (n=3-4). **(I)** Quantification of osteoclast precursor (OCP) percentage ($CD115^{+}Ly6C^{hi}CD11b^{+}CD45^{+}$ cells) in the synovial ankle tissue of 4-OI treated and untreated hTNFtg mice and WT controls (n=3-4). **(J)** Quantification of hypoxia inducible factor 1α (Hif1α) expression in synovial OCPs from 4-OI treated and untreated hTNFtg mice and WT controls, determined by flow cytometry as fold change values of Hif1α mean fluorescence intensity (MFI) gated on OCPs (n=3-4). **(K)** Gating strategy and representative images for flow cytometry analysis of Hif1α expression in synovial OCPs. Data are shown as mean ± SEM. Symbols represent individual mice. P-values were determined by 2-tailed Student´s *t* test for single comparisons and 1-way or 2-way ANOVA for multiple comparisons.

Kachler K, *et al. Ann Rheum Dis* 2024; 83:1691–1706. doi: 10.1136/ard-2023-224774

Supplemental Figures

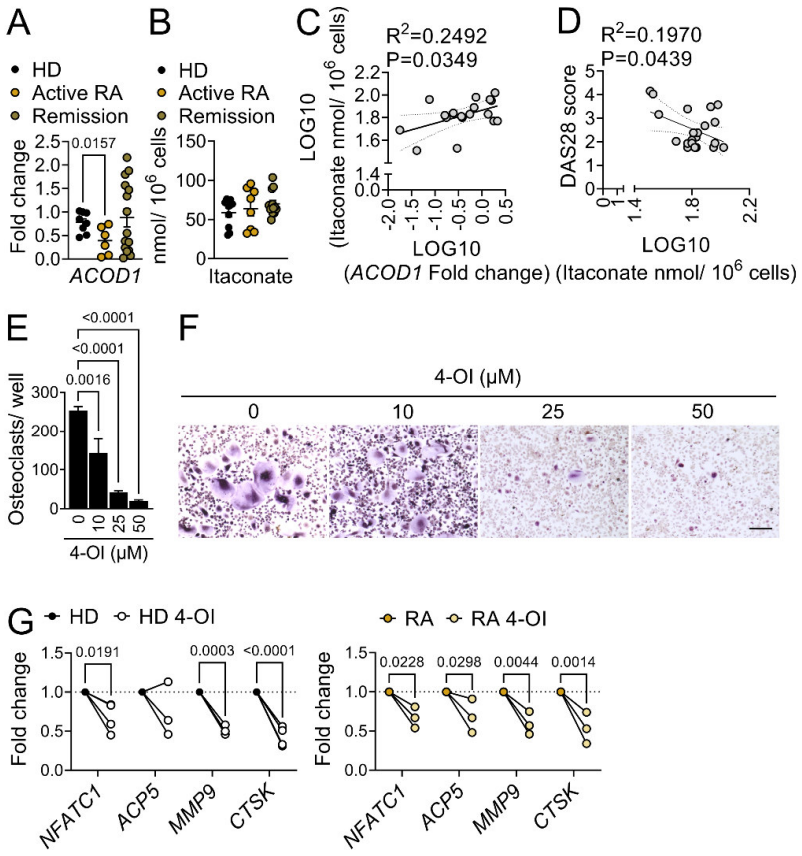

Sup. Fig. 1

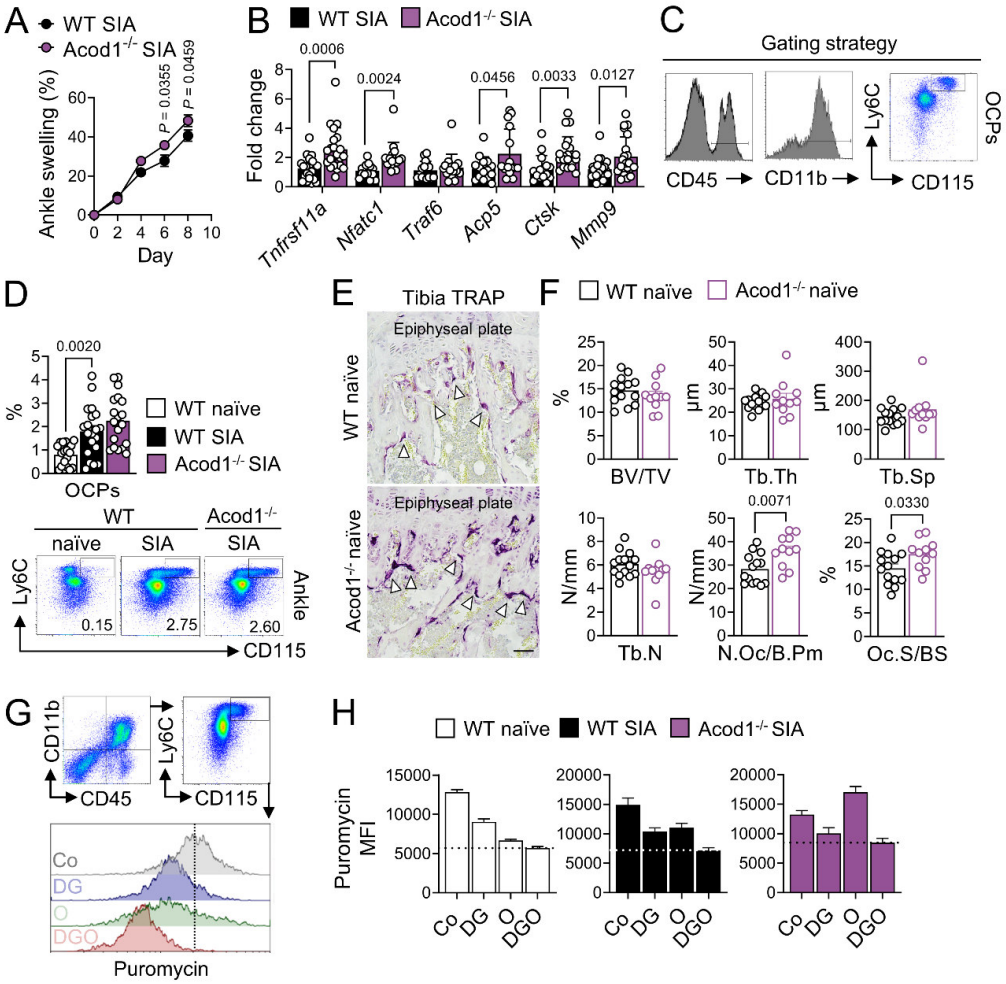
A
WT SIA
Acod1-/- SIA
Ankle swelling (%)
P = 0.0355
P = 0.0459
Day
B
WT SIA
Acod1-/- SIA
Fold change
0.0006
0.0024
0.0456
0.0033
0.0127
Tnfrsf11a
Nfatc1
Traf6
Acp5
Ctsk
Mmp9
C
Gating strategy
CD45
CD11b
Ly6C
CD115
OCPs
D
0.0020
%
OCPs
WT naïve
WT SIA
Acod1-/- SIA
WT
Acod1-/-
naïve
SIA
SIA
Ly6C
CD115
Ankle
0.15
2.75
2.60
E
Tibia TRAP
Epiphyseal plate
WT naïve
Acod1-/- naïve
F
WT naïve
Acod1-/- naïve
%
BV/TV
µm
Tb.Th
µm
Tb.Sp
N/mm
Tb.N
0.0071
N/mm
N.Oc/B.Pm
0.0330
%
Oc.S/BS
G
CD11b
CD45
Ly6C
CD115
Co
DG
O
DGO
Puromycin
H
WT naïve
WT SIA
Acod1-/- SIA
Puromycin MFI
Co
DG
O
DGO

Sup. Fig. 2

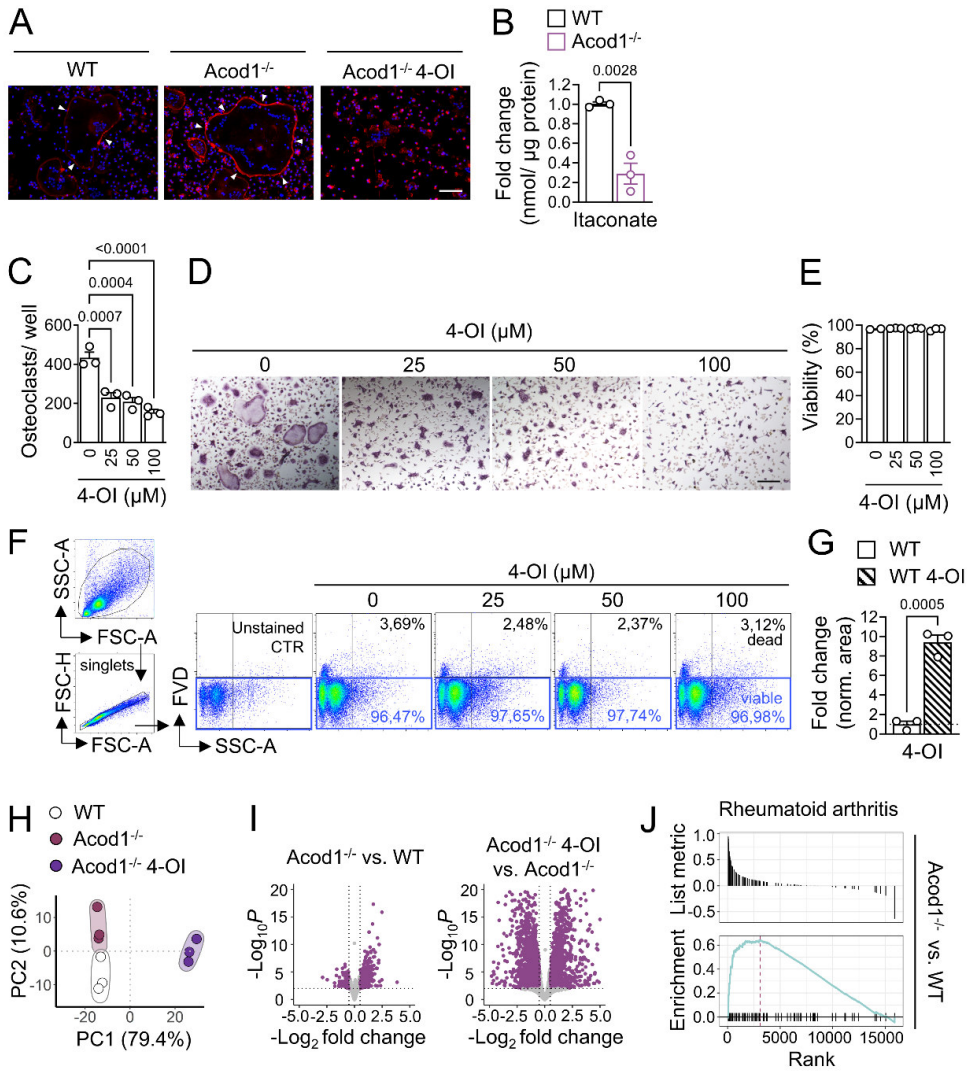
A
WT
Acod1-/-
Acod1-/- 4-OI
B
WT
Acod1-/-
0.0028
Fold change (nmol/ µg protein)
Itaconate
C
<0.0001
0.0004
0.0007
Osteoclasts/ well
4-OI (µM)
D
4-OI (µM)
0
25
50
100
E
Viability (%)
4-OI (µM)
F
SSC-A
FSC-A
FSC-H
singlets
FVD
SSC-A
4-OI (µM)
Unstained CTR
3,69%
2,48%
2,37%
3,12% dead
96,47%
97,65%
97,74%
viable 96,98%
G
WT
WT 4-OI
0.0005
Fold change (norm. area)
4-OI
H
WT
Acod1-/-
Acod1-/- 4-OI
PC2 (10.6%)
PC1 (79.4%)
I
Acod1-/- vs. WT
Acod1-/- 4-OI vs. Acod1-/-
-Log10P
-Log2 fold change
J
Rheumatoid arthritis
List metric
Enrichment
Rank
Acod1-/- vs. WT

Sup. Fig. 3

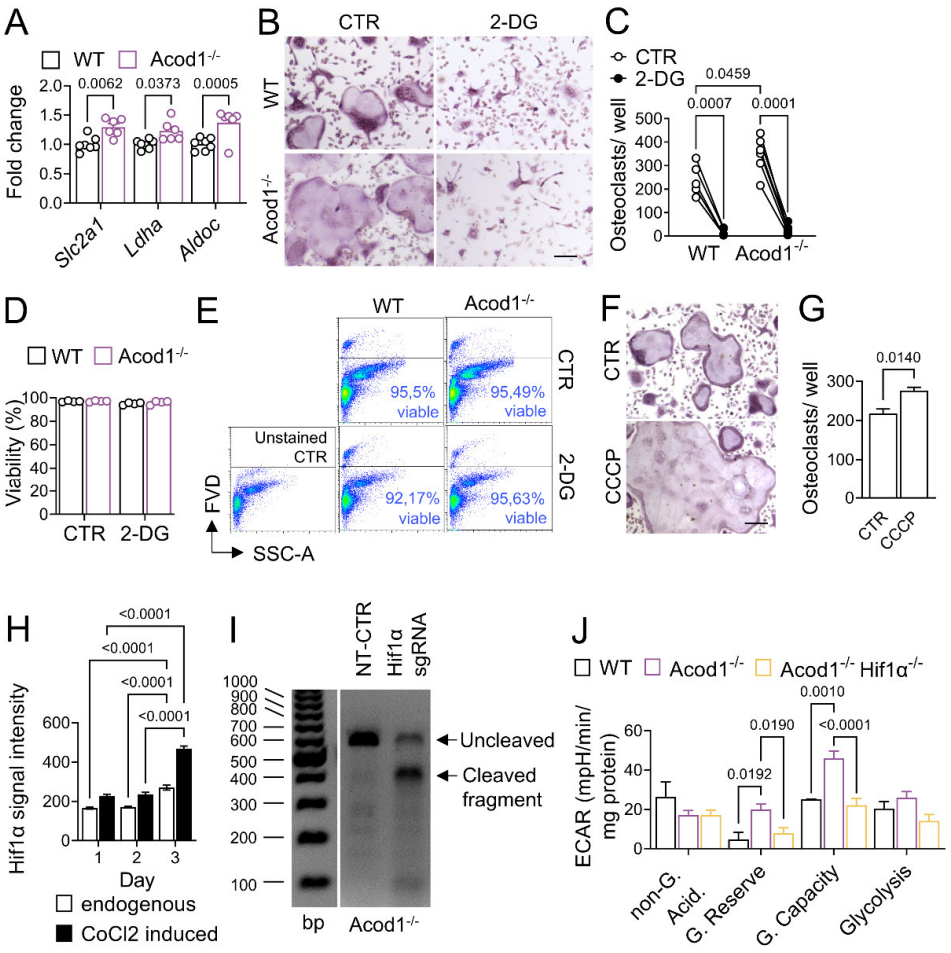
A
WT
Acod1-/-
Fold change
0.0062
0.0373
0.0005
Slc2a1
Ldha
Aldoc
B
CTR
2-DG
WT
Acod1-/-
C
CTR
2-DG
0.0459
0.0007
0.0001
Osteoclasts/ well
WT
Acod1-/-
D
WT
Acod1-/-
Viability (%)
CTR
2-DG
E
WT
Acod1-/-
95,5% viable
95,49% viable
Unstained CTR
92,17% viable
95,63% viable
CTR
2-DG
FVD
SSC-A
F
CTR
CCCP
G
0.0140
Osteoclasts/ well
CTR
CCCP
H
<0.0001
<0.0001
<0.0001
<0.0001
Hif1α signal intensity
Day
endogenous
CoCl2 induced
I
NT-CTR
Hif1α sgRNA
Uncleaved
Cleaved fragment
bp
Acod1-/-
J
WT
Acod1-/-
Acod1-/- Hif1α-/-
0.0010
0.0190
<0.0001
0.0192
ECAR (mpH/min/ mg protein)
non-G. Acid.
G. Reserve
G. Capacity
Glycolysis

Sup. Fig. 4

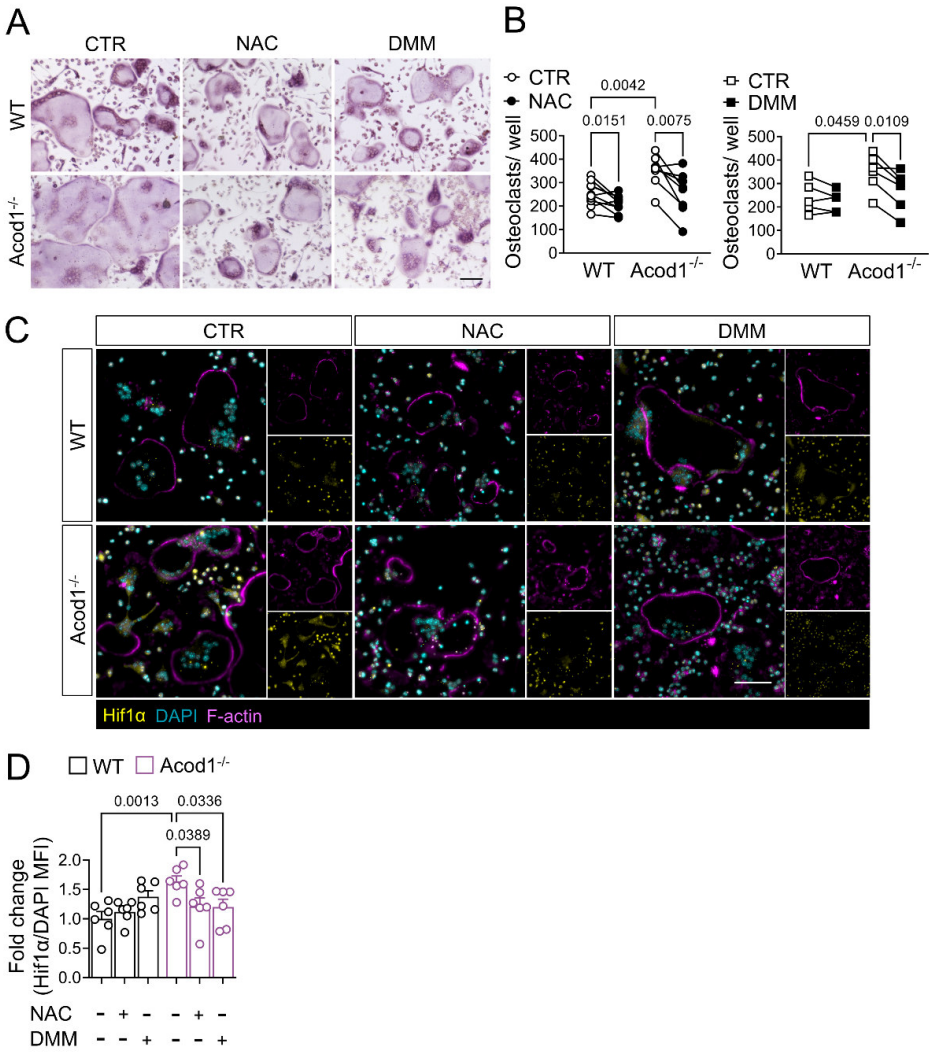
A
CTR
NAC
DMM
WT
Acod1-/-
B
CTR
NAC
0.0042
0.0151
0.0075
Osteoclasts/ well
500
400
300
200
100
0
WT
Acod1-/-
CTR
DMM
0.0459
0.0109
C
CTR
NAC
DMM
WT
Acod1-/-
Hif1α DAPI F-actin
D
WT
Acod1-/-
0.0013
0.0336
0.0389
Fold change (Hif1α/DAPI MFI)
2.0
1.5
1.0
0.5
0.0
NAC - + - - + -
DMM - - + - - +

Sup. Fig. 5

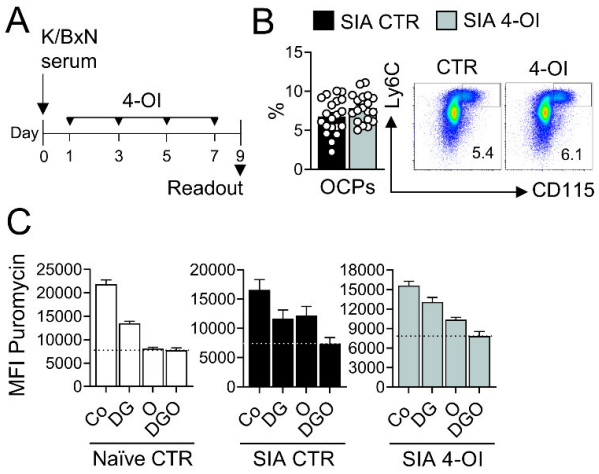
A
K/BxN serum
4-OI
Day
0 1 3 5 7 9
Readout
B
SIA CTR
SIA 4-OI
%
15
10
5
0
OCPs
Ly6C
CTR
4-OI
5.4
6.1
CD115
C
MFI Puromycin
25000
20000
15000
10000
5000
0
20000
15000
10000
5000
0
18000
15000
12000
9000
6000
3000
0
Co
DG
O
DGO
Naïve CTR
SIA CTR
SIA 4-OI

Sup. Fig. 6

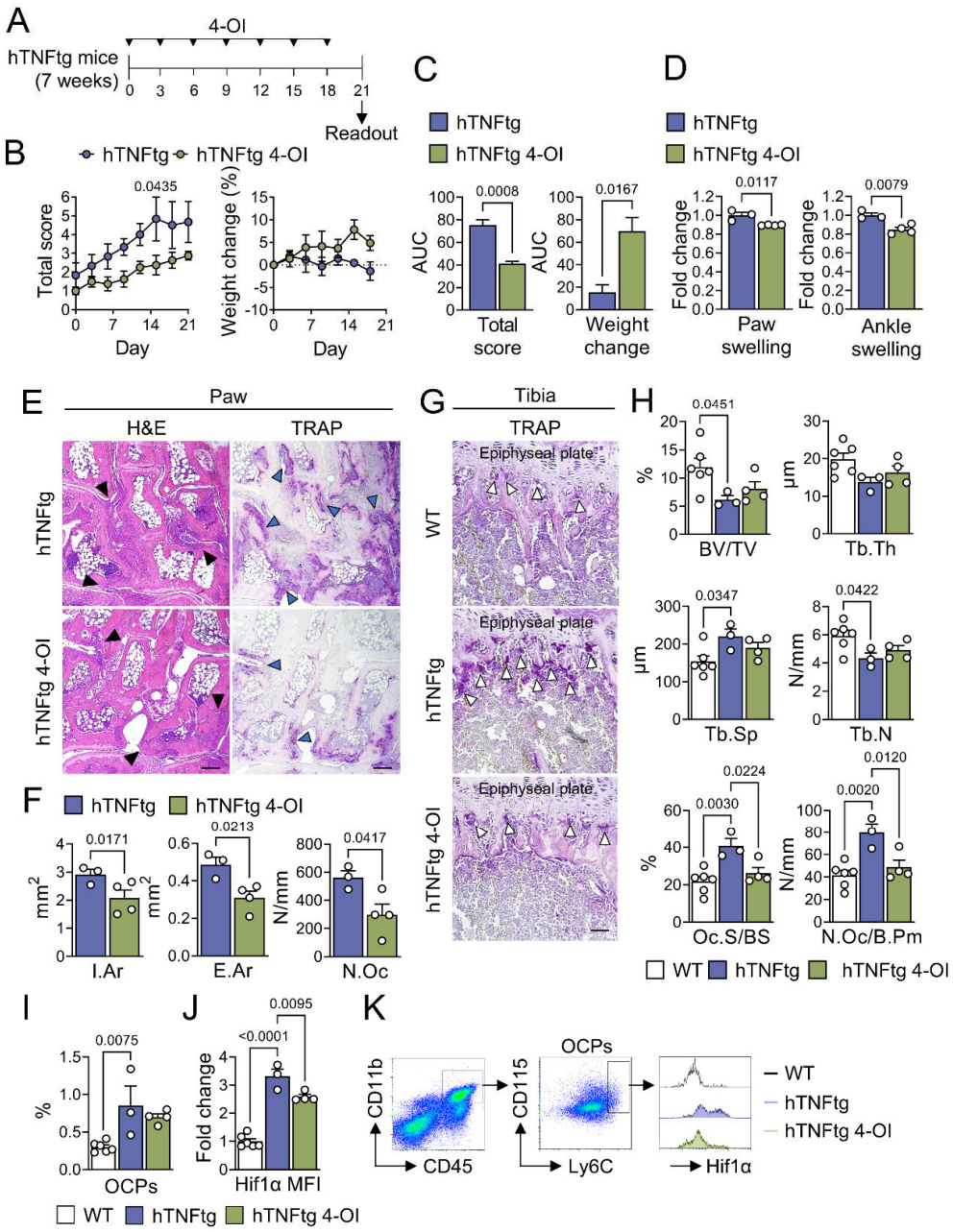
A
4-OI
hTNFtg mice (7 weeks)
0 3 6 9 12 15 18 21
Readout
B
hTNFtg
hTNFtg 4-OI
Total score
Day
Weight change (%)
0.0435
C
AUC
0.0008
0.0167
Total score
Weight change
D
Fold change
0.0117
0.0079
Paw swelling
Ankle swelling
E
Paw
H&E
TRAP
hTNFtg
hTNFtg 4-OI
F
I.Ar
E.Ar
N.Oc
0.0171
0.0213
0.0417
G
Tibia
TRAP
Epiphyseal plate
WT
hTNFtg
hTNFtg 4-OI
H
BV/TV
Tb.Th
Tb.Sp
Tb.N
Oc.S/BS
N.Oc/B.Pm
0.0451
0.0347
0.0422
0.0224
0.0030
0.0120
0.0020
WT
hTNFtg
hTNFtg 4-OI
I
OCPs
0.0075
J
Hif1α MFI
<0.0001
0.0095
K
CD11b
CD45
CD115
Ly6C
OCPs
Hif1α
WT
hTNFtg
hTNFtg 4-OI

Sup. Fig. 7

Supplemental References

1. Gessner A, Muller F, Wenisch P, et al. A Metabolomic Analysis of Sensitivity and Specificity of 23 Previously Proposed Biomarkers for Renal Transporter-Mediated Drug-Drug Interactions. *Clin Pharmacol Ther* 2023;114(5):1058-72. doi: 10.1002/cpt.3017 [published Online First: 20230818]
2. Cao S, Li Y, Song R, et al. L-arginine metabolism inhibits arthritis and inflammatory bone loss. *Ann Rheum Dis* 2024;83(1):72-87. doi: 10.1136/ard-2022-223626 [published Online First: 20240102]
3. Hofmann J, Bornke F, Schmiedl A, et al. Detecting functional groups of Arabidopsis mutants by metabolic profiling and evaluation of pleiotropic responses. *Front Plant Sci* 2011;2:82. doi: 10.3389/fpls.2011.00082 [published Online First: 20111123]